



## Application of fractal modeling to delineate alteration zones and lithological units in Masjed-Daghi Cu-Au porphyry deposit, NW Iran

H. Nikoogoftar Safa and A. Hezarkhani\*

*Department of Mining and Metallurgy Engineering, Amirkabir University of technology (Tehran Polytechnic), Tehran, Iran*

Received 11 May 2018; received in revised form 27 July 2018; accepted 29 July 2018

### Keywords

*Alteration*

*Ordinary Kriging*

*Simple Kriging*

*Concentration-Volume*

*Masjed-Daghi Copper Deposit*

### Abstract

In this paper, we aim to present a quantitative modeling for delineating the alteration zones and lithological units in the hypogene zone of Masjed-Daghi Cu-Au porphyry deposit (NW Iran) based on the drill core data. The main goal of this work is to apply Ordinary Kriging (OK) and concentration-volume (C-V) fractal model based on Cu grades in order to separate the different alteration zones and lithological units. Initially, anisotropy was investigated and modeled based on calculating the experimental semi-variograms of the Cu values, and the main variography directions were identified and evaluated. Then a block model of the Cu grades was generated using the kriging, and the estimation obtained for OK was applied to the C-V fractal model. The C-V log-log plot based on the estimation method represents the various alteration and lithological zones via threshold values. The comparison and interpretation of the alteration zones and lithological units based on the C-V fractal modeling proved that the method was acceptable and capable of correctly delineating the alteration and lithological units. Regarding the correlation derived from log ratio matrix (used to compare the geological model with the C-V fractal results), it was observed that Cu values less than 0.4% were obtained for OK overlapped voxels with the phyllic alteration zone by an overall accuracy (OA) of 0.737. The spatial correlation between the potassic alteration zones resulting from a 3D geological modeling and the high concentration zones in the C-V fractal model based on OK indicated that the alteration zone contained Cu values greater than 0.4% with OA of 0.791. Also using this method, trustworthy results were obtained for the rock units.

### 1. Introduction

The lateral and vertical grade variability is affected by different factors including the rock type and alteration changes [1, 2]. Therefore, delineation of various alteration patterns and investigating their spatial variability is an important task for mining engineers and plays a significant role in grade distribution within porphyry ore deposits. Besides, predicting the spatial distribution of the grade within the porphyry ore deposit helps to better understand these grade-dependent processes [3, 4].

In the past decades, several methods and techniques have been utilized to delineate the alteration zones in hydrothermal including

geological methods based on mineralogical and petrographical assemblages of minerals, geochemical investigations based on thin sections, X-Ray Diffraction (XRD), Electron Probe Micro Analyzer (EPMA), Scanning Electron Microscopy (SEM) and Portable Infrared Mineral Analyzer (PIMA), fluid inclusion studies in porphyry deposits, and investigation of isotope value variation in different zones of porphyry deposits [5-8].

Despite the great practicality and applicability of the mentioned methods, ore grade variability is not considered. Though, porphyry deposits based on grade variations in ore elements significantly

✉ Corresponding author: [ardehez@aut.ac.ir](mailto:ardehez@aut.ac.ir) (A. Hezarkhani).

show zonation [4, 9]. On the other hand, a better geological interpretation of delineation alteration patterns and their spatial variability is obtained by taking the ore element grade values under consideration. Regarding the high importance of the grade in quantitative modeling, selection of a proper estimation method is significantly critical since the fractal/multi-fractal approaches, especially the Concentration-Volume (C-V) modeling, depend on concentration. A proper suitable estimation leads to a better detection of threshold values for an enhanced separation of the alteration zones [10]. In the last three decades, several methods such as geostatistical [11-13] and fractal and multi-fractal techniques [14, 15] have been applied for modeling the spatial variability and distribution of the surveyed uncertain data.

The fractal and multi-fractal theory introduced by Mandelbrot (1982) has been broadly applied in different fields of geoscience such as geochemistry [16-18], geophysics [19-23], structural geology [24-26], ore reserve estimation [27, 28], and remote sensing [29, 30]. Over the last three decades, various fractal and multi-fractal models such as Concentration-Area (C-A) [31-33], Number-Size (N-S) [34-36], Concentration-Distance (C-D) [37], Spectrum-Area (S-A) [38-40], and (C-V) fractal models [41-44] have been widely applied in the mining engineering field. The C-V fractal model proposed by Afzal et al. (2011) is one of the important tools utilized to distinguish various populations with respect to the threshold values [41]. The C-V fractal model is also considered as a proper method to describe the spatial distribution of different attributes within the various ore bodies [42, 43]. In the C-V fractal model, concentration is considered as one of the most important components. Therefore, its accurate estimate is of great importance and enhance delineation of threshold values in the C-V fractal model. Hence, selecting a proper estimation method is considerably critical for the C-V modeling, which behaves towards detection of threshold values for separation of alteration zones and rock units [10].

Geostatistical tools have been considered as a powerful technique for the spatial modeling of reservoir heterogeneities, predicting spatial attributes, and the purpose of uncertainty. The application of the mentioned technique has increased significantly since 1990s [44-46]. The kriging method, as a geostatistical interpolation technique, is an optimal and linear unbiased spatial estimator that minimize the variance [47].

The underlying assumption of geostatistics is that both the mean and covariance are stationary. The geostatistical methodology begins with two major steps, i.e. structural analysis and kriging. Over the past 50 years, many researchers have used various geostatistical methods for ore grade modelling including simple kriging (SK), ordinary kriging (OK), lognormal kriging, indicator kriging, co-kriging, universal kriging, residual kriging, moving window regression residual kriging, disjunctive kriging, and stochastic simulation such as sequential Gaussian simulation (SGS) and Sequential Indicator Simulation (SIS) [48, 49].

This article follows two goals. At first, OK and SK are applied to estimate the block model of Cu grades in hypogene zone of Masjed-Daghi Cu-Au porphyry deposit in NW Iran, and the results obtained are compared. Secondly, the OK and C-V fractal modelings are used to delineate the alteration zones and rock units in the hypogene zone of the case study.

The rest of the paper is organized as what follows. In Section 2, the regional geology, geological setting, and alteration of the case study are described. In Section 3, the borehole dataset and statistical calculations are described. The overview of the methods and their principles, advantages, and limitations are drawn in Section 4. In Section 5, the results obtained are discussed. Finally, in Section 6, conclusions are presented.

## 2. Case study

Porphyry copper deposits (PCDs), as the most important copper sources, include nearly three-fourths of the world's copper [50]. The various igneous rocks such as quartz monzonite (e.g. Butte, Montana deposit), diorite (e.g. Caspiche, Chile deposit), granodiorite (e.g. Cananea, Mexico deposit), quartz diorite (e.g. Miduk, Iran deposit), andesite, dacite, and monzonite are the most commonly reported rock types hosting PCDs [51-54].

PCDs are generally located in the Urumieh-Dokhtar Magmatic Belt (MDMB) in Iran (Figure 1), formed during the subduction of Arabian plate under central Iran in alpine orogeny era [55, 56]. MDMB hosts the largest known PCDs of Iran including Sungun and Sar-Cheshmeh, which are currently mined and located in NW and SE parts of this tectonic belt, respectively. These economic deposits are associated with mid to late Miocene diorite/granodiorite to quartz-monzonite stocks (Figure 1) [57, 58].

The Sungun porphyry stock is located in the Oligocene–Miocene rocks. They intruded to the Cretaceous carbonate and Eocene volcano-sedimentary rocks [2]. This economic deposit comprises more than 900 Mt ore at grade of 0.76% Cu and 0.06% Mo. The Sar-Cheshmeh porphyry that belongs to Miocene era intruded to Eocene andesite, and consists of 1,200 Mt ore at an average grade of 0.64% Cu, 0.27 g/t Au, 3.9 g/t Ag, and 0.03% Mo [57, 58]. Moreover, in the central part of this belt, many deposits of porphyry, and epithermal systems such as Miduk, Gor-Gor or Kahang, Sari Gunay, Dalli, Agh-Darreh, Zar-Shuran, Darreh- Zerrshk,

Ali-Abad, and South Ardestan deposits can be found (Figure 1) [59-62].

Masjed-Daghi, as a case study here, is located at Julfa sheet (1:100,000 series) in NW of Iran. The area is composed of a very likely gold mineralization bearing epithermal mineralization, which appears to be associated with a porphyry Cu–Mo system at deeper levels [63, 64]. This exploration area, which seems to be prone to porphyry and/or epithermal mineralization, is located at the northern latitudes 38°52'03"–38°53'03" and eastern longitudes 45°56'03"–45°58'28" in Julfa sheet. The geological investigations and prospects in Masjed-Daghi area have started since 2003 [63, 64].

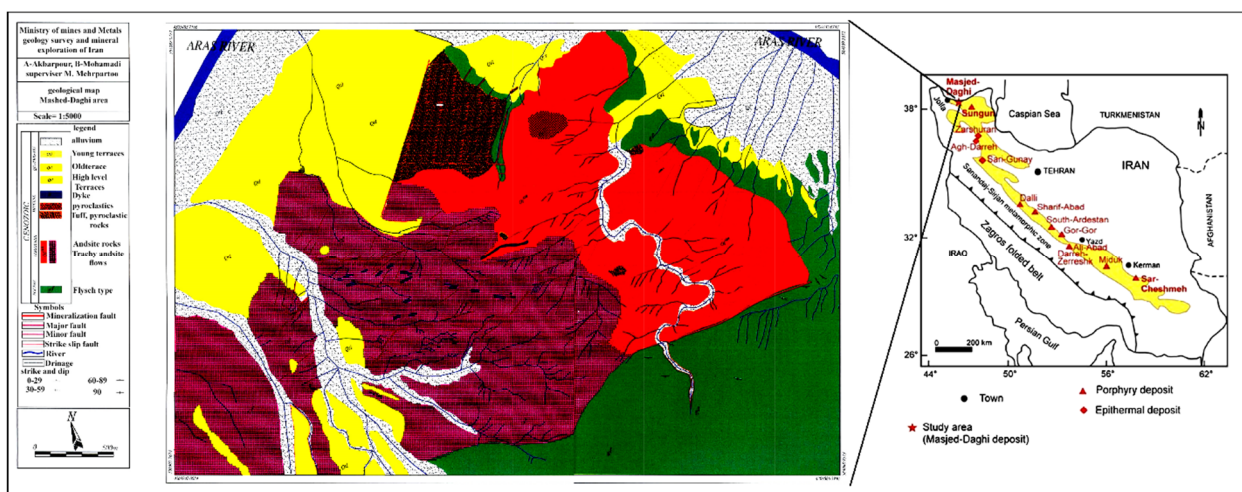


Figure 1. Location of the porphyry and epithermal ore deposits at MDMB in Iran [63], and the geological map of Masjed–Daghi area in scale 1:5,000 [63, 64].

## 2.1. Geology and mineralization

The oldest observed rock units in this case study belong to the Eocene flysch-type sediments, and the other outcrops mainly involve Oligocene volcanic rocks with andesitic to trachyandesitic compositions. They are intruded by a shallow quartz monzonite porphyry intrusion (Figure 1). The studied area consists of the Cenozoic and Quaternary rocks. The rock units are as follow: Eocene flysch, andesite, trachyandesite, dacite, rhyodacite, Oligocene agglomerate, and Quaternary deposits as traces, sand dune, and river flood sediments [63, 64]. During the Pyrenean phase, igneous rocks injected into the flysch sediments of Eocene, and then Azerbaijan plate was broken by intensive movements in Miocene [63, 64], though the extrusion of magma is also possible (Figure 1). Previous research works have reported the existence of the gold, copper, lead, and zinc mineralization in this area. The Masjed–Daghi deposit is PDs, and associated with medium

sulfidation copper–gold veins and veinlets [63, 64]. Genetically, this deposit is related to magmatic-hydrothermal, and in term of paragenesis, it is associated with minerals such as chalcopyrite, barite, malachite, azurite, galena, and gold. The maximum and average amount of Au in the silicic veins is 40 and 2.5 g/ton, respectively, within 1 ton tonnage [63, 64]. The minerals such as pyrite, chalcopyrite, molybdenite, sphalerite, galena, and Fe oxides in brecciated quartz and quartz–barite veins as well as stockworks associated with porphyry system are possible locations to mineralization. In the Masjed-Daghi exploration area, the epithermal system is related to a porphyry Cu–Mo system in deeper levels. This claim is confirmed by the occurrence of phyllic and potassic alterations as well as the abundant contents of Cu (1,000 to >10,000 ppm) and Mo (50–400 ppm) observed in the samples from drill cores and sparse trenches [63, 64].

### 3. Borehole dataset

The borehole dataset plays an important role in geoscience investigations in both mineral exploration and grade estimation. A total of 50 boreholes were drilled in the studied area, 16 of which belonged to the pre-drilled boreholes (BH series) with a total length of 1882.3 m, and 34 boreholes were related to MAD series boreholes with a total length of 15015.95 m (Figure 2). The dataset included the collars, lithology, down-hole survey, and assay. The other acquired data were zone, alteration, mineral, and recovery. The dataset for assay was analyzed by the ICP-MS method at the Zarazma laboratory, Tehran. Based on the mineralogical, geological, and geochemical results, it was found that the case study was favorable for the mineralization of Cu. The data was validated and subjected to the statistical analysis. The histogram and descriptive statistics of copper grades from 8267 samples in the hypogene zone of the case study are shown in Figures 3 and 4 and Table 1. The statistical parameters of Cu grade based on lithology and alteration in the hypogene zone of the case study are also shown in Tables 2 and 3, respectively. Accordingly, two lithology units consist of diorite and andesite, and two alteration zones composed of potassic and phyllic account for more than 90% of the data length. The Cu regionalized variable was modeled by a second-order stationary random function. There was no trend of Cu concentration

in any direction; this means that Cu concentration does not depend on the coordinates of samples (Figures 5(a-c)). Consequently, assumptions of the stationary function are tenable.

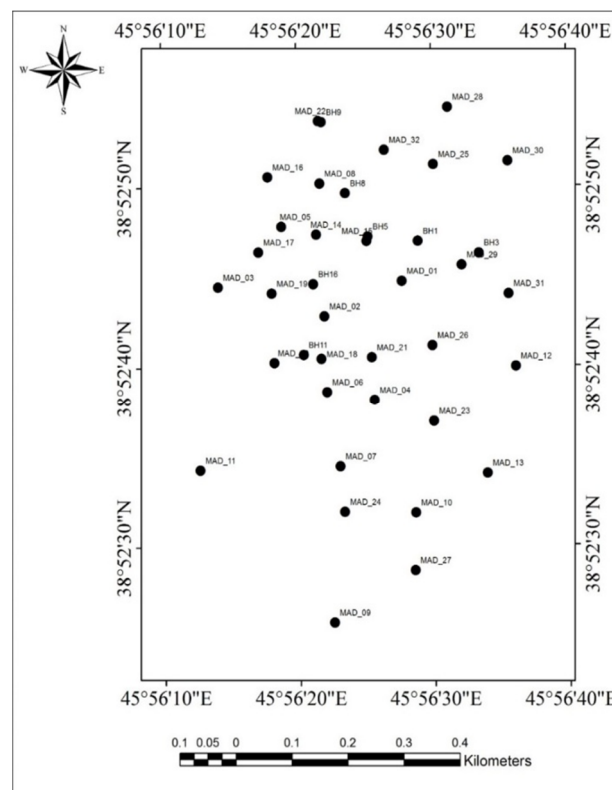


Figure 2. Borehole location map of Masjed-Daghi deposit.

Table 1. Statistical parameters of Cu element in boreholes (raw values).

Element	Detection limit	Length	Min.	Max.	Mean	Variance	St. deviation	Skewness	Kurtosis
Cu	1 ppm	16898.25	0	2.37	0.21	0.03	0.17	1.56	5.13

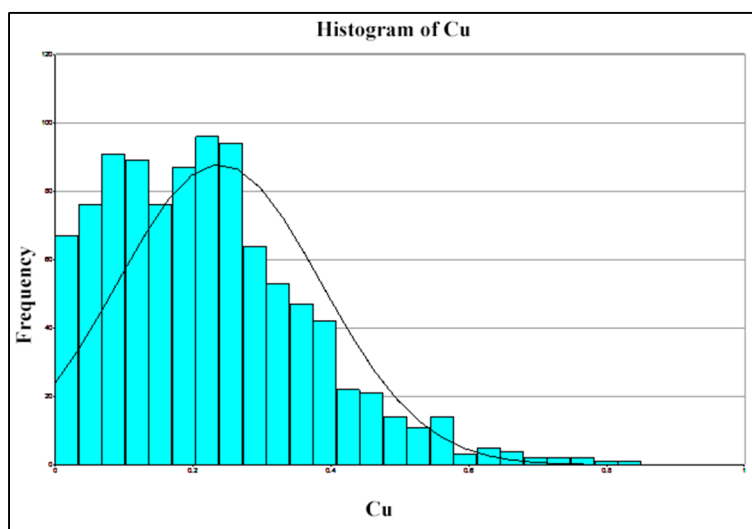


Figure 3. Histogram of the raw data in the hypogene zone of Masjed-Daghi deposit.

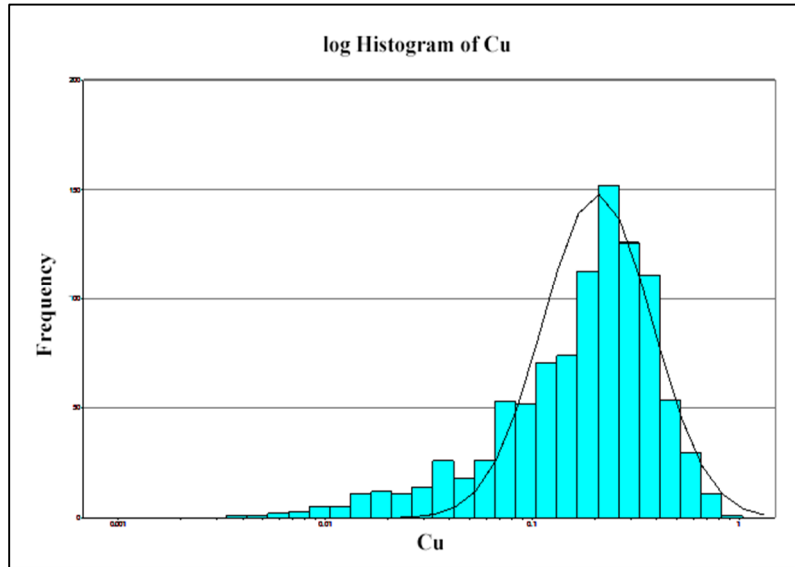
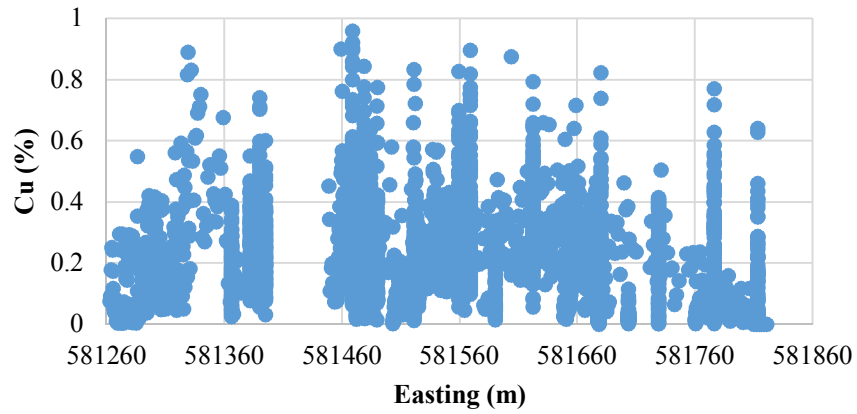
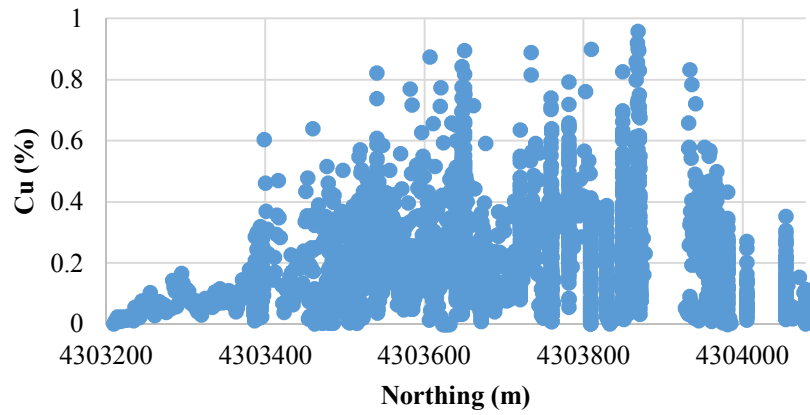


Figure 4. Histogram of the regularized data in the hypogene zone of Masjed-Daghi deposit.

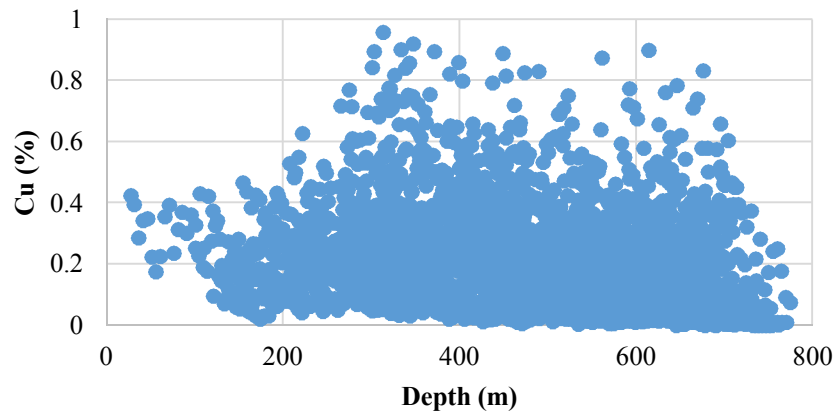


(a)



(b)

Figure 5. Variability of Cu concentration in (a) east–west direction, (b) north–south direction, and (c) depth within the hypogene zone of Masjed-Daghi deposit.



(c)  
Figure 5. Continued.

Table 2. The statistical parameters of Cu grade based on lithology in the hypogene zone.

ROCK type	Length	Length%	Cu		
			Min.	Max.	Mean
ALL	653.7	3.86	0	0.31	0.06
ANS	<b>4836.2</b>	<b>28.61</b>	<b>0</b>	<b>1.04</b>	<b>0.16</b>
CLS	491.5	2.90	0.03	1.22	0.34
DAC	364.3	2.15	0.003	0.45	0.05
<b>DIO</b>	<b>10499.05</b>	<b>66.028</b>	<b>0</b>	<b>2.37</b>	<b>0.24</b>
NA	8	0.047	0.018	0.018	0.018
QZL	29.4	0.17	0.01	0.504	0.14
TUF	16.1	0.095	0.009	0.023	0.013

ANS = Andesite, ALL = Alluvium, DAC = Dacite, DIO = Diorite, TUF = Tuff, QZL = Quartzolite, CLS = Core Loss.

Table 3. The statistical parameters of Cu grade based on alteration in the hypogene zone.

Alteration type	Length	Length%	Cu		
			Min.	Max.	Mean
ARG	84.3	0.49	0.072	0.784	0.325
CHL	44	0.26	0.02	0.1	0.058
NA	1151.45	6.81	0	1.22	0.15
<b>PHY</b>	<b>3705.9</b>	<b>21.93</b>	<b>0</b>	<b>1.04</b>	<b>0.158</b>
<b>POT</b>	<b>9847.45</b>	<b>58.32</b>	<b>0</b>	<b>1.38</b>	<b>0.248</b>
PRP	16.1	0.09	0.009	0.023	0.0137
SER	8.4	0.04	0.181	0.419	1.246
SLC	158.35	0.93	0.007	0.93	0.134
BLANK	1882.3	11.13	0.001	2.37	0.14

ARG = Argillic; CAL = Calcified; CHL = Chloritic; PHY = Phyllic; POT = Potassic; PRP = Propylitic; SLC = Silicified; NA = Not Applicable.

## 4. Methodology

### 4.1. Geostatistics

Over the past decades, different methods of spatial interpolation have been presented by numerous researchers. These methods are mostly related together and have similar principles. The spatial interpolation models are categorized into two classes: (a) mechanical/deterministic and (b) statistical/probability. The mechanical models are based upon empirical parameters, which include techniques such as Inverse Distance Interpolation (IDW) and Splines. The error estimation is not considered in such methods. In contrast, the parameters of the statistical/probability techniques

are estimated based on probability principals and considered the error estimation. Kriging is one of the most important statistical/probability models, which is based on the “theory of regionalized variables” [65, 66]. The kriging technique consists of two basic steps. The first step is the estimation of the semi-variogram by sample training data, given by:

$$\gamma(h) = \frac{1}{2.n(h)} \sum_{i=1}^{n(h)} \{z(i) - z(i+h)\}^2 \quad (1)$$

where  $\gamma(h)$  is the estimated semi-variance,  $n(h)$  is the number of pairs observed  $[z(i), z(i+h)]$ , and  $h$

is the distance between the pairs. The second step is predicting at unknown spatial coordinates through a linear combination of measured values shown by:

$$z^*(x_0) = \sum_{i=1}^n \lambda_i \cdot z(x_i) \tag{2}$$

where  $z^*(x_0)$  is the estimated value for any  $x_0$  location,  $n$  is the number of measured values  $z(i)$ ,  $z(x_i)$  is the value involved in the estimation, and  $\lambda_i$  is the attached weight to each measured value  $z(i)$ . The best estimator is always unbiased and has a minimum variance. Therefore, the kriging system is deduced as:

$$\sum_{j=1}^n \lambda_j \cdot \gamma(x_i, x_j) = \mu + \gamma(x_i, x_0) \tag{3}$$

where  $\gamma(x_i, x_0)$  is the semi-variance function of a vector with an origin at  $x_i$  and extremity at  $x_0$ ;  $\gamma(x_i, x_j)$  is the semi-variance function of a vector with an origin at  $x_i$  and extremity at  $x_j$ ; and  $\mu$  is the Lagrange multiplier [66].

#### 4.1.1. Simple kriging (SK)

The average value of the entire dataset is used in SK. The details of SK have been given by Journel and Huijbregts. The estimation of SK based on Eq. (1) is calculated by Eq. (4):

$$\hat{z}(x_0) = \sum_{i=1}^n \lambda_i Z(x_i) + \left[ 1 - \sum_{i=1}^n \lambda_i \right] \mu \tag{4}$$

where  $\mu$  is the stationary mean, which is assumed constant over the whole domain and calculated as the average of the data. This estimator is utilized to assess residuals from this reference value given a priori, and therefore, it is referred to as “kriging with known mean”. The number of sampled points used to make the estimation in Eq. (4) is determined by the range of influence of the semi-variogram. It is not necessarily 0, as the lack of bias condition  $\left[ 1 - \sum_{i=1}^n \lambda_i \right]$  in SK; the greater the value of  $\left[ 1 - \sum_{i=1}^n \lambda_i \right]$ , the more the estimator will be drawn toward the mean; in general, the value of  $\left[ 1 - \sum_{i=1}^n \lambda_i \right]$  increases in relatively poor sampled regions. The second-order stationary is assumed in SK, which is constant mean, variance, and covariance over the domain or the region of

interest. OK (no a priori mean) is most often used because such an assumption is too restrictive [67-69].

#### 4.1.2. Ordinary kriging (OK)

OK is the standard and most frequently used estimation technique in ore grade prediction. The observational data of a variogram model, which is interpreted from all the data within the area, is used in this method to estimate a value at a non-sampled location in a region of interest. OK is also applied to estimate the block grades. Ordinary block kriging implicitly calculates the mean in a moving neighborhood, while minimizes the error under the second-order stationary assumption [70-72].

In mathematical terms, OK is a spatial interpolation estimator  $\hat{Z}(x_0)$  that is applied to find the best linear unbiased estimation of a second-order stationary random field with an unknown constant mean, as follows:

$$\hat{Z}(x_0) = \sum_{i=1}^n \lambda_i Z(x_i) \tag{5}$$

where  $\hat{Z}(x_0)$  is the kriging estimation at a non-sampled location  $x_0$ ;  $Z(x_0)$  is the sampled value at location  $x_i$ ; and  $\lambda_i$  is the weight factor of  $Z(x_i)$ . The estimation error is Eq. (6):

$$\hat{Z}(x_0) - Z(x_0) = R(x_0) = \sum_{i=1}^N \lambda_i Z(x_i) - Z(x_0) \tag{6}$$

where  $Z(x_0)$  is an unknown true value at  $x_0$  and  $R(x_0)$  is the estimation error. For an unbiased estimator, the mean value of the estimation error must be equal to zero. Therefore,

$$E\{R(x_0)\} = 0 \tag{7}$$

and

$$\sum_{i=1}^N \lambda_i = 1 \tag{8}$$

For solving the interpolation problem by kriging, the minimum variance of the estimation error is required [72, 73].

#### 4.2. C-V fractal method

The C-V fractal model was first developed from 2D C-A fractal model to 3D by Afzal et al. (2011). This model separates various mineralization zones in order to characterize the distribution of major, minor, and trace element concentrations in relation to the Iranian Cu

porphyry deposits [41]. The general formula is as follows (Eq. (9)):

$$V(\rho \leq v) \propto r^{-\alpha_1}; V(\rho \geq v) \propto r^{-\alpha_2} \quad (9)$$

where  $V(\rho \leq v)$  and  $V(\rho \geq v)$  represent the volumes with concentration values ( $\rho$ ) less than or equal to and greater than or equal to the contour values ( $v$ ); and  $\alpha_1$  and  $\alpha_2$  are the characteristic exponents. In the log-log plots of concentration contours versus volumes, certain concentration contours representing breakpoints in the plots are considered the threshold values separating geochemical populations in the data [42, 43].

## 5. Result and discussion

### 5.1. Results of OK and SK

The data described in Section 3 was used to estimate the Cu grade. However, prior to the kriging calculations, it was necessary to carry out a series of data preprocessing. The first task in dealing with data preprocessing is to determine

and treat the high-grade values designated as outliers. These values dramatically impact statistical analysis and interpretation. Outlier high-grade values may transform a mineral occurrence into an economic mineral deposit, and might be sufficient to justify the development of a mining project [74]. There are various methods available to mitigate and control the impact of the high grade data on the resource estimation. In this work, the box plot and probability plot (Figure 6) was used to remove outliers [75]. Composite is another significant issue in data preprocessing. Moreover, using equal support (volume) samples is an important matter in estimation. That is why the data was composited to equal lengths [76]. Here, the data for Masjed-Daghi resource analysis by OK was taken from 2 m composites. The lowest loss length was obtained regarding this composite length, while the Cu grade and variance of Cu were similar to the original data.

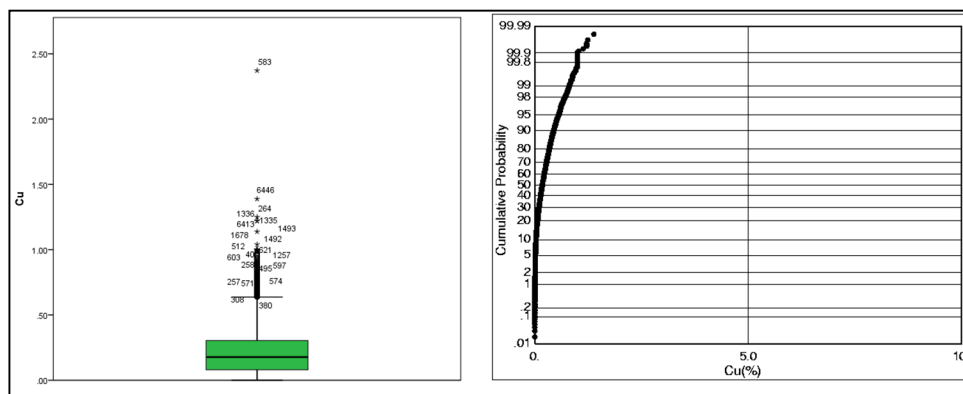


Figure 6. Box plot (left) and probability plot (right) used to remove outliers.

#### 5.1.1. Variography

The data variography for OK and SK is the next step after data preprocessing. Considering the random spatial variation and randomness, the variogram function reflects the structure of spatial variability of a regionalized variable. Variogram is then the best method available to describe the spatial dependencies in a covariance stationary process.

Mineralization is considered anisotropic due to the different behaviors in every direction. Consequently, it is necessary to conduct individual analyses in multiple directions to determine the correct spatial structure. As the experimental variograms display various behaviors in different directions, an anisotropic variogram model is required to be fitted to them. In general, the variogram has directional properties in more than one dimension. The variography is carried out using Data mine

Software.

An omnidirectional semi-variogram of raw data along azimuth of 00°, Plunge of 00°, spread of 90°, and lag spacing of 40 m follows a spherical model with a nugget effect of 0.052 (%)<sup>2</sup>, which reaches a sill of 0.020 (%)<sup>2</sup> at a range of 204 m (Figure 7-a). In order to investigate anisotropy, directional semi-variograms are calculated and modelled considering different directions with 30° horizontal angular increments, 15° horizontal angular tolerance, 30° vertical angular increments, and 15° vertical angular tolerance in the hypogene zone of porphyry ore deposit. The ore deposit contains anisotropy because most of the variograms are in different ranges. The main directions resulting from variography for 3 main directions of the search ellipsoid are presented in Figures 7(b)-(d). The parameters of the directional semi-variogram model are shown in Table 4.



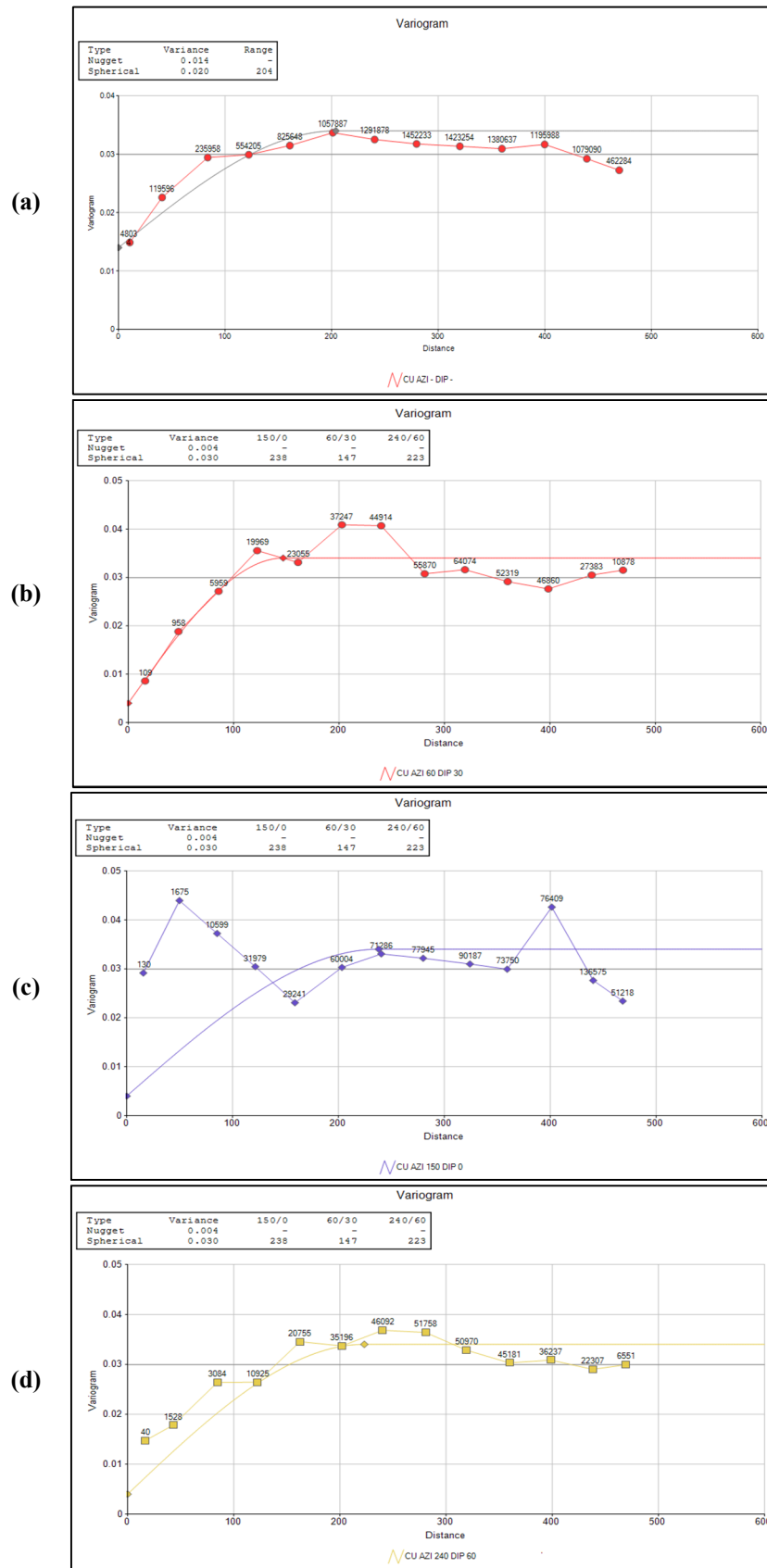


Figure 7. Experimental semi-variogram and appropriate fitted model of (a) omnidirectional semi-variograms and (b) directional semi-variograms with Azimuth = 60; Dip = 30 (c) directional semi-variograms with Azimuth = 150; Dip = 0 (d) directional semi-variograms with Azimuth = 240; Dip = 60 for 3 main directions of the search ellipsoid in the hypogene zone of Masjed-Daghi deposit.

**Table 4. Parameters of the directional semi-variogram for 3 main directions of the search ellipsoid in the hypogene zone of Masjed-Daghi deposit.**

Variogram model	Azimuth	Dip	nugget effect (%) <sup>2</sup>	Range (m)	Threshold (%) <sup>2</sup>
Spherical	60	30	0.004	147	0.030
Spherical	150	0	0.004	238	0.030
Spherical	240	60	0.004	223	0.030

In order to validate the fitted model to the hypogene zone variogram, the cross-validation method was applied. The correlation coefficient of the estimated and actual values was equal to 80%, which is acceptable.

**5.1.2. Results of SK and OK**

The theory of methods was applied to the Masjed-Daghi copper deposit in order to verify the practical efficacy of OK and SK to estimate un-sampled location values. To estimate Cu%, the OK and SK methods were used to get estimations at points on a grid 10 m × 10 m × 10 m. The estimation and 3D modeling process was started from the elevation of 0 to 800 m above the sea level in the mine. The start levels in the east and north directions were from 581113 to 582043 m

and from 4303279 to 4304159 m, respectively. The estimation of SK for Cu concentration in different elevations (above the sea level) is shown in Figure 8. In addition, the estimation of OK for Cu concentration in different elevations is also shown in Figure 9.

A 3D modeling of the grade in an ore deposit has lots of advantages. Therefore, the robust evaluations and judgments about different parts of the ore deposit depend on a careful execution of the process. The 3D model of Cu grade by the SK and OK methods in the Masjed-Daghi copper deposit are shown in Figures 10 and 11, respectively. These models were generated by Data mine Software Package.

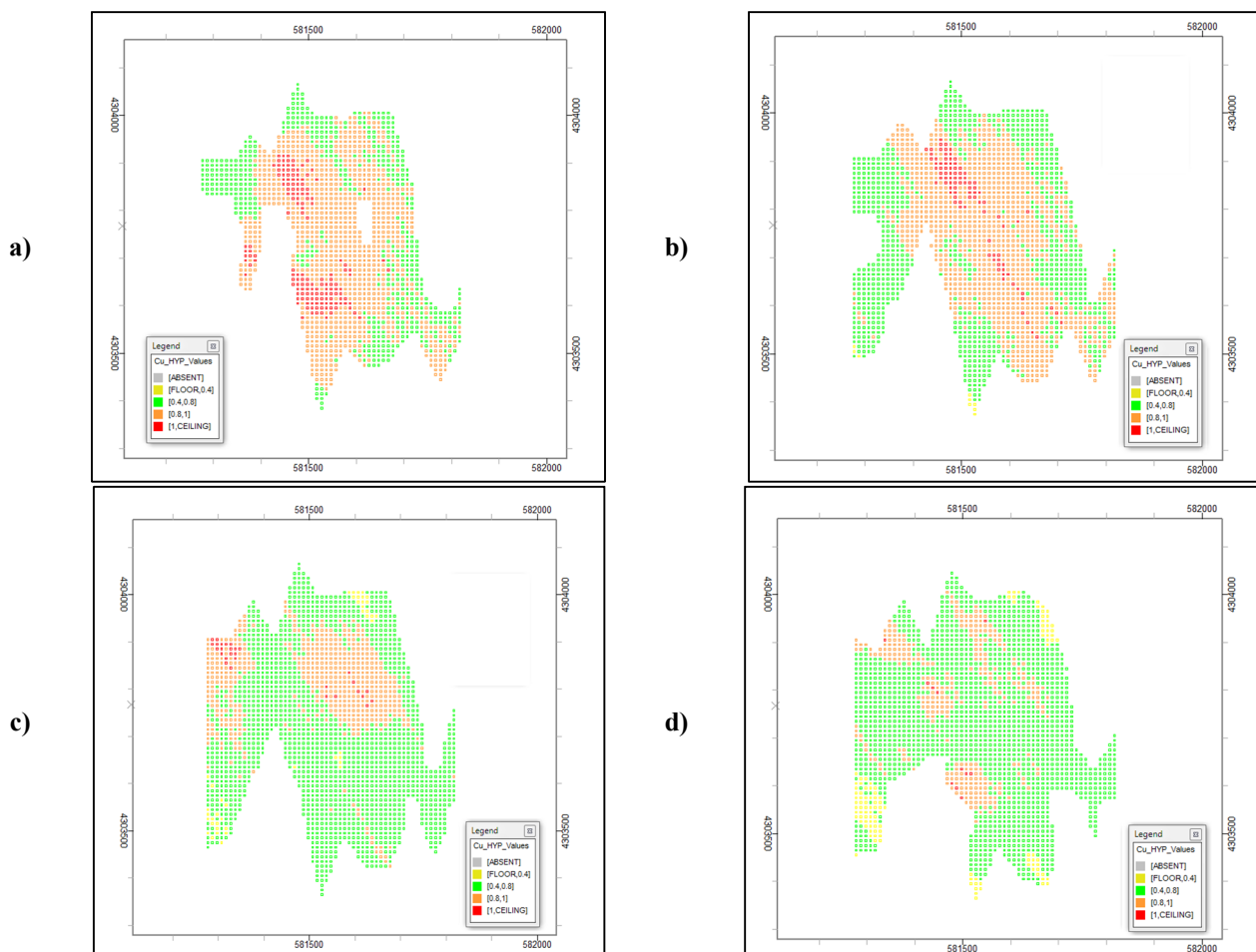


**Figure 8. SK estimation for Cu concentration in elevation a) z = 300, b) z = 400, c) z = 500, and d) z = 600 m in Masjed-Daghi copper deposit.**

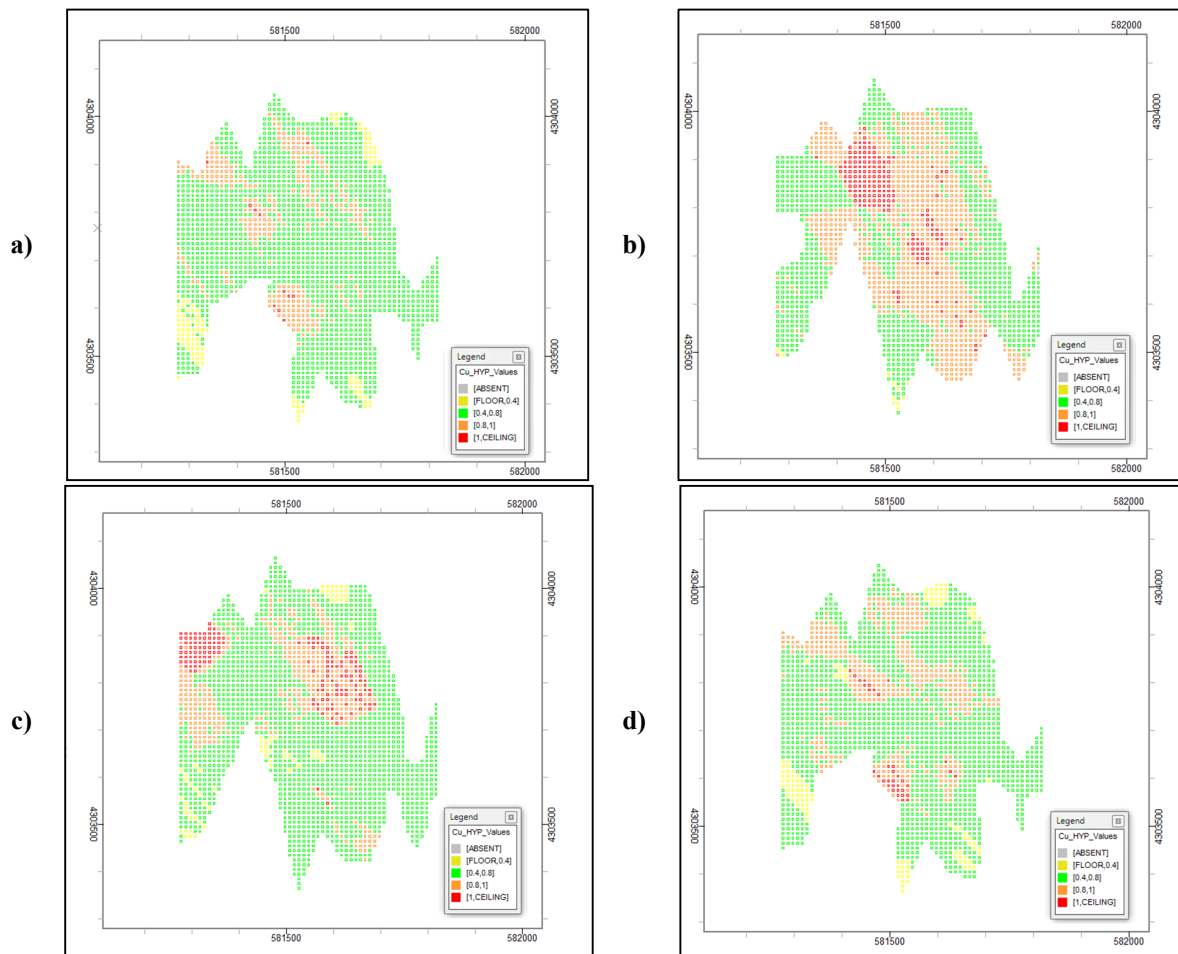


Figure 9. OK estimation for Cu concentration in elevation a)  $z = 300$ , b)  $z = 400$ , c)  $z = 500$ , and d)  $z = 600$  m in Masjed-Daghi copper deposit.

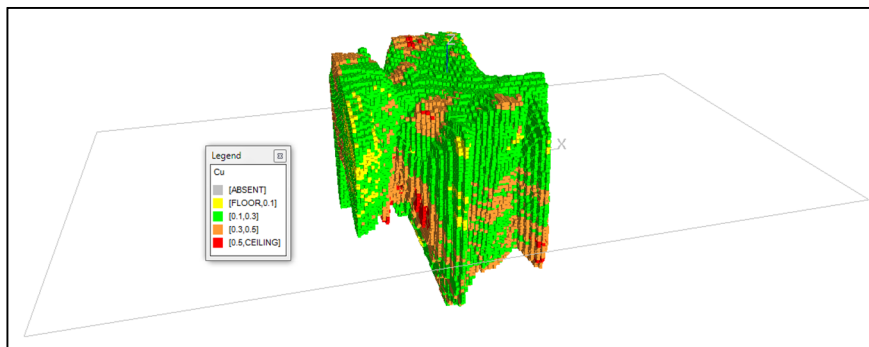


Figure 10. 3D model of the estimations of Cu concentration by SK in Masjed-Daghi copper deposit.

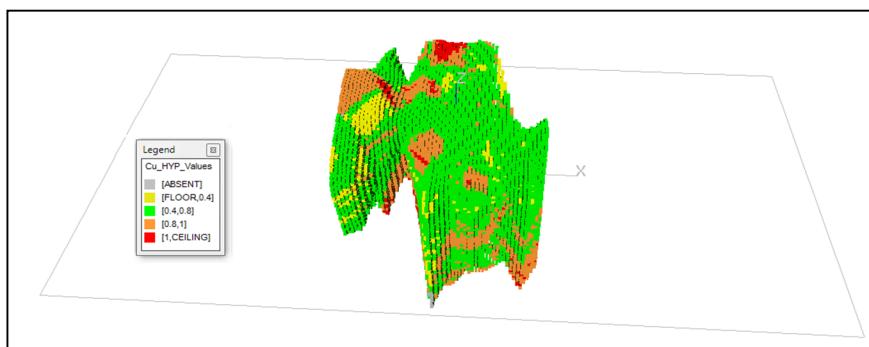


Figure 11. 3D model of the estimations of Cu concentration by OK in Masjed-Daghi copper deposit.

The statistical calculations carried out showed that the mean concentration of Cu (%) in the original data was 0.269 (%). The mean value of SK was 0.267 (%) in comparison with the mean value of OK that was 0.272 (%). The resulting estimations by the SK method were near the average concentration of Cu (%) in the original data. In addition, the minimum value for the OK estimator was 0.0036 (%) as against 0.005 (%) in the case of the SK methods. The maximum values for OK and SK were 1.383 (%) and 1.22 (%), respectively. It means that simple kriging overestimates the low true value and underestimates the high true value. On the other hand, SK tries to gather all the estimations near the mean value without considering the spatial data structures, although there is more similarity between the OK estimations and true values. As a result, SK is less accurate than OK. Consequently, the model obtained by OK is more accurate, and a future economic decision by its results is more reliable.

**5.2. Results of C-V fractal model**

The C-V fractal model is considered as a proper method to describe the spatial distribution of different attributes (ore elements in this scenario) within the various ore bodies. Using the 3D model of Cu distribution obtained from OK in the porphyry ore deposit, the C-V log-log plot was calculated (Figure 12). The data pairs of the concentrations and volumes were projected to the log-log graphs, and linear regression was applied to fit straight lines. The coefficient of

determination  $R^2$  ( $0 \leq R^2 \leq 1$ ) was calculated to evaluate the effect of linear regression. The regression line was established via adjusting it to achieve the largest coefficient of determination. Consequently, one threshold value and two population values were obtained (Table 5).

The alteration and lithological models play key roles in zone delineation and also in presenting the geological models. Potassic alteration in the Lowell and Guilbert model is the host of the high grade Cu mineralization, and is located in the central part of the Cu porphyry deposits [1]. Moreover, rocks such as diorite are also the host of the high grade Cu mineralization. The 3D geological model of alteration zones and geological units generated by the geological drill core data in the Data mine v.3.24 software are shown in Figures 13 and 14, respectively.

In order to calculate the spatial correlation between two binary models, especially the mathematical and geological ones, the logratio matrix [77] was applied. Comparison between the C-V fractal model results, the geological model of the alteration zones and the lithological units were carried out to obtain the number of overlapped voxels (A, B, C, and D). Type I error (T1E), Type II error (T2E), and overall accuracy (OA) of different fractal populations were estimated for each alteration zone using the obtained numbers [77]. The results obtained were tabulated in Tables 6-9.

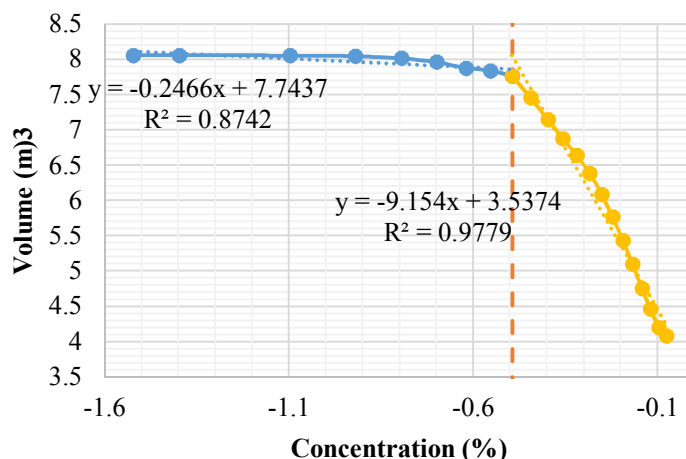


Figure 12. C-V fractal log-log plot resulting from OK modeling within the hypogene zone.

Table 5. Cu threshold values identified using the C-V fractal modeling for the OK results.

Population	Cu (%) threshold value (OK)
Population 1	$0 \leq \text{Cu} (\%) < 0.4$
Population 2	$0.4 \leq \text{Cu} (\%) < 1.38$

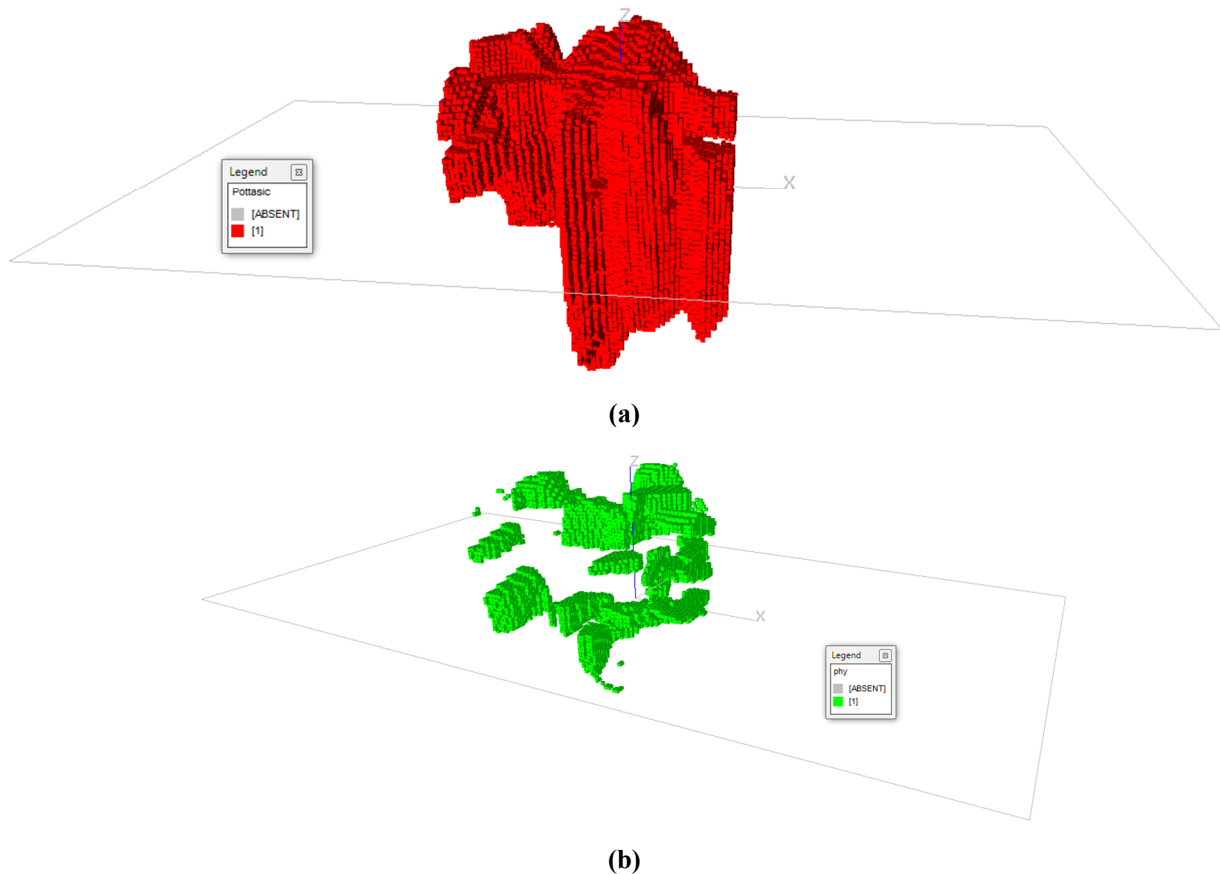


Figure 13. Alteration in the hypogene zone of Masjed-Daghi based on the geological model: a) potassic and b) phyllic.

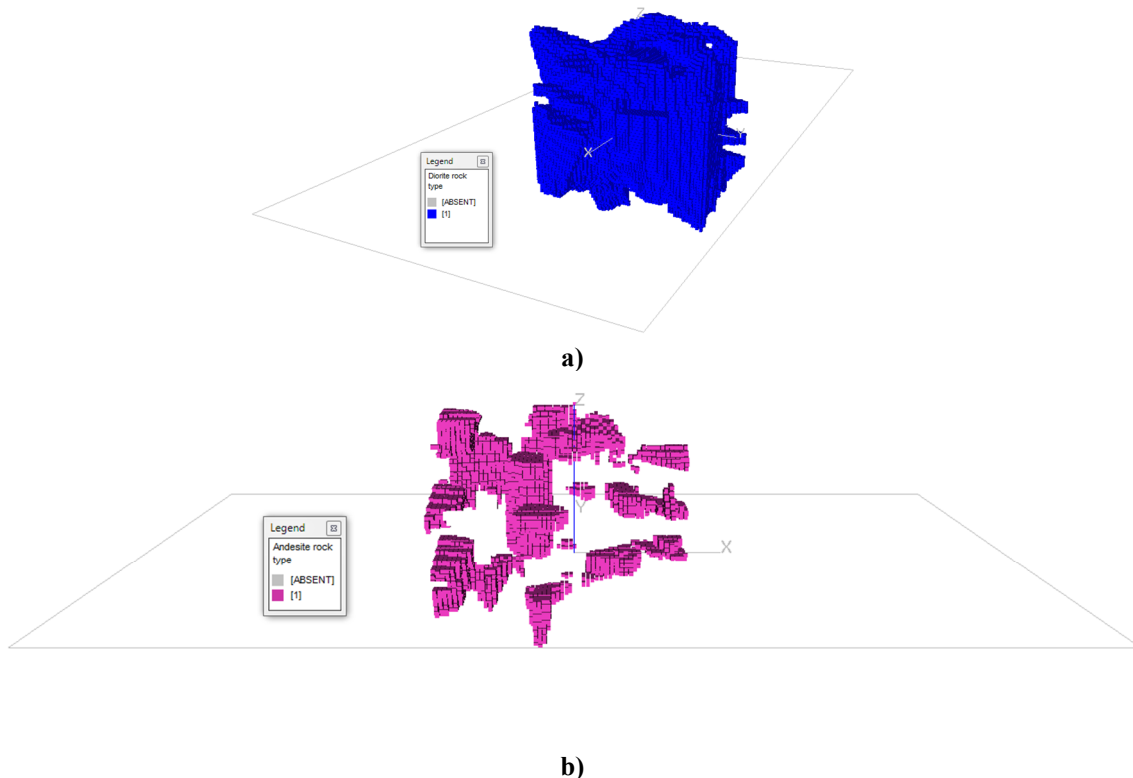


Figure 14. Rock units in the hypogene zone of Masjed-Daghi based on the geological model: a) Diorite, b) Andesite.

**Table 6. OA, T1E, and T2E resulting from the comparison between the potassic alteration zone in the 3D geological model and the threshold values of Cu in the C–V fractal model obtained for the hypogene zone.**

		Potassic alteration of geological model			
Fractal model	Inside zone	Inside zone		Outside zone	
	Outside zone	True positive (A)	False negative (C)	False positive (B)	True negative (D)
		Type I Error = $C/(A + C)$		Type II Error = $B/(B + D)$	
		Overall accuracy = $(A + D)/(A + B + C + D)$			
		Potassic alteration of geological model			
C–V fractal model ( $0.4 \leq Cu$ )	Inside zones	Inside zones		Outside zones	
	Outside zones	A	46531	B	25279
		C	14455	D	103353
		T1E	0.237	T2E	0.196
		OA	0.791		

**Table 7. OA, T1E, and T2E resulting from the comparison between the phyllic alteration zone in the 3D geological model and the threshold values for Cu in the C–V fractal model obtained for the hypogene zone.**

		Phyllic alteration of geological model			
C–V fractal model ( $0 < Cu < 0.4$ )	Inside zones	Inside zones		Outside zones	
	Outside zones	A	46479	B	35305
		C	14489	D	93361
		T1E	0.237	T2E	0.274
		OA	0.737		

**Table 8. OA, T1E, and T2E resulting from the comparison between the Diorite unit in the 3D geological model and the threshold values for Cu in the C–V fractal model obtained from the hypogene zone.**

		Diorite lithology of geological model			
C–V fractal Model ( $0.4 \leq Cu$ )	Inside zones	Inside zones		Outside zones	
	Outside zones	A	6839	B	64971
		C	1155	D	103390
		T1E	0.144	T2E	0.386
		OA	0.625		

**Table 9. OA, T1E, and T2E resulting from the comparison between the Andesite unit in the 3D geological model and the threshold values for Cu in the C–V fractal model obtained from the hypogene zone.**

		Andesite lithology of geological model			
C–V fractal model ( $0.4 \leq Cu$ )	Inside zones	Inside zones		Outside zones	
	Outside zones	A	6547	B	75255
		C	1447	D	93398
		T1E	0.181	T2E	0.446
		OA	0.566		

## 6. Conclusions

In order to delineate the spatial structures of ore zones, the geological models should be constructed based on the borehole data. Ore grades are not usually considered in the conventional methods, while variations in this parameter are the most obvious and salient features. Uncertainty occurs in logging a drill core, alteration, and rock unit recognition during the geological study, and in the correlation detected between the grade distribution and alteration, and rock unit patterns. This reveals that ore grades can be used to find the spatial structure of alteration zones and rock units. The

quantitative model that was produced in this process resulted in a qualitative model of alterations and rock units. In order to construct this model, multiple mathematical analyses such as the kriging estimation and the C-V fractal models can be used. Mathematical tools such as the OK and C-V fractal models were applied together in this work to separate different alteration zones and rock units in the hypogene zone of the Masjed-Daghi Cu-Au porphyry deposit, NW Iran. At first, the applicability of OK for ore grade estimation was examined. The outcome was compared with SK. SK produced a result that was smoother, and the results obtained

showed that simple kriging could be less accurate than ordinary kriging. The model obtained by ordinary kriging was found to be more accurate, and a future economic decision by ordinary kriging results was more reliable. Then the estimation obtained for OK was applied to the C-V fractal model. Implementing the C-V fractal modeling on the results derived from OK led to the separation of different grade populations, and consequently, different alteration zones and rock units. According to the correlation derived from the log ratio matrix, which was used to compare the geological model and quantitative modeling obtained from the C-V fractal model and OK, showed that Cu values less than 0.4% obtained for OK had overlapped voxels with the phyllic alteration zone by an overall accuracy (OA) of 0.737. The spatial correlation between the potassic alteration zones resulting from 3D geological modeling and the high concentration zones in the C-V fractal model based on OK indicated that the alteration zone contained Cu values greater than 0.4% with OA of 0.791. As expected, the models obtained supported the Lowell-Guilbert (1970) [1] model of alteration zones in the porphyry copper deposits. Also trustworthy results were obtained for rock units using this method.

## References

- [1]. Lowell, J.D. and Guilbert, J.M. (1970). Lateral and vertical alteration-mineralization zoning in porphyry ore deposits. *Economic Geology*. 65: 373-408.
- [2]. Hezarkhani, A. and Williams-Jones, A.E. (1998). Controls of alteration and mineralization in the Sungun porphyry copper deposit, Iran; evidence from fluid inclusions and stable isotopes. *Economic Geology*. 93: 651-670.
- [3]. Asghari, O., Hezarkhani, A. and Soltani, F. (2009). The comparison of alteration zones in the Sungun porphyry copper deposit, Iran (based on fluid inclusion studies). *Acta Geologica Polonica*. 59: 93-109.
- [4]. Soltani, F., Afzal, P. and Asghari, O. (2014). Delineation of alteration zones based on Sequential Gaussian Simulation and concentration-volume fractal modeling in the hypogene zone of Sungun copper deposit, NW Iran. *Journal of Geochemical Exploration*. 140: 64-76.
- [5]. Schwartz, G.M. (1947). Hydrothermal alteration in the "porphyry copper" deposits. *Economic Geology*. 42: 319-352.
- [6]. Beane, R. (1982). Hydrothermal alteration in silicate rocks. University of Arizona Press, Tucson. pp. 117-137.
- [7]. Roedder, E. (1971). Fluid inclusion studies on the porphyry-type ore deposits at Bingham, Utah, Butte, Montana, and Climax, Colorado. *Economic Geology*. 66: 98-118.
- [8]. Nash, J.T. (1976). Fluid-inclusion petrology data from porphyry copper deposits and applications to exploration: a summary of new and published descriptions of fluid inclusions from 36 porphyry copper deposits and discussion of possible applications to exploration for copper deposits. US Govt.
- [9]. Afzal, P., Alghalandis, Y.F., Moarefvand, P., Omran, N.R. and Haroni, H.A. (2012). Application of power-spectrum-volume fractal method for detecting hypogene, supergene enrichment, leached and barren zones in Kahang Cu porphyry deposit, Central Iran. *Journal of Geochemical Exploration*. 112: 131-138.
- [10]. Afzal, P., Madani, N., Shahbeik, S. and Yasrebi, A.B. (2015). Multi-Gaussian kriging: a practice to enhance delineation of mineralized zones by Concentration-Volume fractal model in Dardevey iron ore deposit, SE Iran. *Journal of Geochemical Exploration*. 158: 10-21.
- [11]. Emery, X. and Gonzalez, K.E. (2007). Incorporating the Uncertainty in Geological Boundaries into Mineral Resources Evaluation. *Geological Society of India*. 69: 29-38.
- [12]. Chiles, J.P. and Delfiner, P. (2009). *Geostatistics: modeling spatial uncertainty*. John Wiley & Sons.
- [13]. Rossi, M.E. and Deutsch, C.V. (2013). *Mineral resource estimation*. Springer Science & Business Media.
- [14]. Cheng, Q., Xu, Y. and Grunsky, E. (2000). Integrated spatial and spectrum method for geochemical anomaly separation. *Natural Resources Research*. 9: 43-52.
- [15]. Zuo, R., Cheng, Q. and Xia, Q. (2009). Application of fractal models to characterization of vertical distribution of geochemical element concentration. *Journal of Geochemical Exploration*. 102: 37-43.
- [16]. Mandelbrot, B.B. (1982). *The fractal geometry of nature*. San Francisco, CA.
- [17]. Carranza, E.J.M., Zuo, R. and Cheng, Q. (2012). Fractal/multifractal modelling of geochemical exploration data. *Journal of Geochemical Exploration*. 122: 1-3.
- [18]. Zuo, R. and Wang, J. (2016). Fractal/multifractal modeling of geochemical data: a review. *Journal of Geochemical Exploration*. 164: 33-41.
- [19]. Turcotte, D. (1989). A fractal approach to probabilistic seismic hazard assessment. *Tectonophysics*. 167: 171-177.

- [20]. Abedi, M., Torabi, S.A. and Norouzi, G.H. (2013). Application of fuzzy AHP method to integrate geophysical data in a prospect scale, a case study: Seridune copper deposit. *Bollettino di Geofisica Teorica ed Applicata*. 54(2).
- [21]. Wang, W., Zhao, J. and Cheng, Q. (2013). Application of singularity index mapping technique to gravity/magnetic data analysis in southeastern Yunnan mineral district. China. *Journal of Applied Geophysics*. 92: 39-49.
- [22]. Dimri, V.P. and Srivastava, R.P. (2005). Fractal modeling of complex subsurface geological structures. In *Fractal Behaviour of the Earth System* (pp. 23-37). Springer, Berlin, Heidelberg.
- [23]. Chen, G., Cheng, Q., Liu, T. and Yang, Y. (2013). Mapping local singularities using magnetic data to investigate the volcanic rocks of the Qikou depression, Dagang oilfield, eastern China. *Nonlinear processes in geophysics*. 20: 501-511.
- [24]. Korvin, G. (1992). *Fractal models in the earth sciences*. Elsevier Science Ltd.
- [25]. Pérez-López, R. and Paredes, C. (2006). On measuring the fractal anisotropy of 2-D geometrical sets: Application to the spatial distribution of fractures. *Geoderma*. 134: 402-414.
- [26]. Hodkiewicz, P., Weinberg, R., Gardoll, S. and Groves, D. (2005). Complexity gradients in the Yilgarn Craton: fundamental controls on crustal-scale fluid flow and the formation of world-class orogenic-gold deposits. *Australian Journal of Earth Sciences*. 52: 831-841.
- [27]. Wang, Q., Deng, J., Zhao, J., Liu, H., Wan, L. and Yang, L. (2010). Tonnage-cutoff model and average grade-cutoff model for a single ore deposit. *Ore Geology Reviews*. 38: 113-120.
- [28]. Ford, A. and Blenkinsop, T.G. (2009). An expanded de Wijs model for multifractal analysis of mineral production data. *Mineralium Deposita*. 44(2): 233.
- [29]. Martinez, P., Schertzer, D. and Pham, K. (1997). Texture modelisation by multifractal processes for SAR image segmentation.
- [30]. Spirintseva, O.V. (2016). An application of multifractal analysis to photogrammetric image segmentation. *Data Stream Mining & Processing (DSMP)*. IEEE First International Conference on IEEE. pp. 286-289.
- [31]. Cheng, Q., Agterberg, F. and Ballantyne, S. (1994). The separation of geochemical anomalies from background by fractal methods. *Journal of Geochemical Exploration*. 51: 109-130.
- [32]. Cheng, Q., Agterberg, F. and Bonham-Carter, G. (1996). A spatial analysis method for geochemical anomaly separation. *Journal of Geochemical Exploration*. 56: 183-195.
- [33]. Cheng, Q. (1999). Spatial and scaling modelling for geochemical anomaly separation. *Journal of Geochemical exploration*. 65: 175-194.
- [34]. Sadeghi, B., Moarefvand, P., Afzal, P., Yasrebi, A.B. and Saein, L.D. (2012). Application of fractal models to outline mineralized zones in the Zaghia iron ore deposit. Central Iran. *Journal of Geochemical Exploration*. 122: 9-19.
- [35]. Deng, J., Wang, Q., Wan, L., Yang, L., Gong, Q., Zhao, J. and Liu, H. (2009). Self-similar fractal analysis of gold mineralization of Dayingezhuang disseminated-veinlet deposit in Jaodong gold province, China. *Journal of Geochemical Exploration*. 102: 95-102.
- [36]. Turcotte, D.L. (2002). Fractals in petrology. *Lithos*. 65: 261-271.
- [37]. Li, C., Ma, T. and Shi, J. (2003). Application of a fractal method relating concentrations and distances for separation of geochemical anomalies from background. *Journal of Geochemical Exploration*. 77: 167-175.
- [38]. Cheng, Q. (2007). Multifractal imaging filtering and decomposition methods in space, Fourier frequency, and Eigen domains. *Nonlinear Processes in Geophysics*. 14: 293-303.
- [39]. Xu, Y. and Cheng, Q. (2001). A fractal filtering technique for processing regional geochemical maps for mineral exploration. *Geochemistry: Exploration, environment, analysis*. 1: 147-156.
- [40]. Panahi, A., Cheng, Q. and Bonham-Carter, G.F. (2004). Modelling lake sediment geochemical distribution using principal component, indicator kriging and multifractal power-spectrum analysis: a case study from Gowganda, Ontario. *Geochemistry: Exploration, Environment, Analysis*. 4: 59-70.
- [41]. Afzal, P., Alghalandis, Y.F., Khakzad, A., Moarefvand, P. and Omran, N.R. (2011). Delineation of mineralization zones in porphyry Cu deposits by fractal concentration-volume modeling. *Journal of Geochemical Exploration*. 108: 220-232.
- [42]. Yasrebi, A.B., Afzal, P., Wetherelt, A., Foster, P. and Esfahanipour, R. (2013). Correlation between geology and concentration-volume fractal models: significance for Cu and Mo mineralized zones separation in the Kahang porphyry deposit (Central Iran). *Geologica Carpathica*. 64: 153-163.
- [43]. Delavar, S.T., Afzal, P., Borg, G., Rasa, I., Lotfi, M. and Omran, N.R. (2012). Delineation of mineralization zones using concentration-volume fractal method in Pb-Zn carbonate hosted deposits. *Journal of Geochemical Exploration*. 118: 98-110.
- [44]. Reis, A., Sousa, A. and Fonseca, E.C. (2003). Application of geostatistical methods in gold



geochemical anomalies identification (Montemor-O-Novo, Portugal). *Journal of Geochemical Exploration*. 77: 45-63.

[45]. Benndorf, J. and Dimitrakopoulos, R. (2013). Stochastic long-term production scheduling of iron ore deposits: Integrating joint multi-element geological uncertainty. *Journal of Mining Science*. 49: 68-81.

[46]. Pyrcz, M.J. and Deutsch, C.V. (2014). *Geostatistical reservoir modeling*. Oxford university press.

[47]. Marinoni, O. (2003). Improving geological models using a combined ordinary-indicator kriging approach. *Engineering Geology*. 69: 37-45.

[48]. Badel, M., Angorani, S. and Panahi, M.S. (2011). The application of median indicator kriging and neural network in modeling mixed population in an iron ore deposit. *Computers & geosciences*. 37: 530-540.

[49]. Tahmasebi, P. and Hezarkhani, A. (2012). A hybrid neural networks-fuzzy logic-genetic algorithm for grade estimation. *Computers & geosciences*. 42: 18-27.

[50]. Sillitoe, R.H. (2010). Porphyry copper systems. *Economic geology*. 105: 3-41.

[51]. Barton, M.D., Staude, J., Zürcher, L. and Megaw, P.K. (1995). Porphyry copper and other intrusion-related mineralization in Mexico. *Porphyry copper deposits of the American Cordillera: Arizona Geological Society Digest*. 20: 487-524.

[52]. John, D., Ayuso, R., Barton, M., Blakely, R., Bodnar, R., Dilles, J., Gray, F., Graybeal, F., Mars, J. and McPhee, D. (2010). Porphyry copper deposit model, chap. B of *Mineral deposit models for resource assessment*. US Geological Survey Scientific Investigations Report. 169 P.

[53]. Rusk, B.G., Reed, M.H. and Dilles, J.H. (2008). Fluid inclusion evidence for magmatic-hydrothermal fluid evolution in the porphyry copper-molybdenum deposit at Butte, Montana. *Economic Geology*. 103: 307-334.

[54]. Sillitoe, R.H., Tolman, J. and Van Kerkvoort, G. (2013). Geology of the Caspiche porphyry gold-copper deposit, Maricunga Belt, northern Chile. *Economic Geology*. 108: 585-604.

[55]. Berberian, M. and King, G. (1981). Towards a paleogeography and tectonic evolution of Iran. *Canadian journal of earth sciences*. 18: 210-265.

[56]. Pourhosseini, F. (1983). Petrogenesis of Iranian plutons, a study of Natanz and Bazman intrusive complexes. Rep./Iran. Geol. survey.

[57]. Hezarkhani, A. (2006). Alteration/mineralization and controls of chalcopyrite dissolution/deposition in the Raigan porphyry system, Bam-Kerman, Iran. *International Geology Review*. 48: 561-572.

[58]. Shahabpour, J. (1982). Aspects of alteration and mineralization at the Sar-Cheshmeh copper-molybdenum deposit. University of Leeds.

[59]. Asadi, H., Voncken, J., Kühnel, R. and Hale, M. (2000). Petrography, mineralogy and geochemistry of the Zarshuran Carlin-like gold deposit, northwest Iran. *Mineralium Deposita*. 35: 656-671.

[60]. Taghipour, N., Aftabi, A. and Mathur, R. (2008). Geology and Re-Os Geochronology of Mineralization of the Miduk Porphyry Copper Deposit, Iran. *Resource Geology*. 58: 143-160.

[61]. Richards, J.P., Wilkinson, D. and Ullrich, T. (2006). Geology of the Sari Gunay epithermal gold deposit, northwest Iran. *Economic Geology*. 101: 1455-1496.

[62]. Boomeri, M., Nakashima, K. and Lentz, D.R. (2009). The Miduk porphyry Cu deposit, Kerman, Iran: A geochemical analysis of the potassic zone including halogen element systematics related to Cu mineralization processes. *Journal of Geochemical Exploration*. 103: 17-29.

[63]. Akbarpour, A., Gholami, N., Azizi, H. and Torab, F.M. (2013). Cluster and R-mode factor analyses on soil geochemical data of Masjed-Daghi exploration area, northwestern Iran. *Arabian Journal of Geosciences*. 6: 3397-3408.

[64]. Farjandi, F., Faiziev, A., Fozilov, M., Bastani, H. and Soleimani, S. (2013). The application of biogeochemistry for gold exploration in the Masjed-Daghi, Julfa, NW Iran. *Arabian Journal of Geosciences*. 6: 1435-1446.

[65]. Dai, F., Zhou, Q., Lv, Z., Wang, X. and Liu, G. (2014). Spatial prediction of soil organic matter content integrating artificial neural network and ordinary kriging in Tibetan Plateau. *Ecological Indicators*. 45: 184-194.

[66]. Isaaks, E. and Srivastava, R. (1989). *Applied geostatistics: An introduction*. Applied geostatistics: An introduction to.

[67]. Li, C., Lu, Z., Ma, T. and Zhu, X. (2009). A simple kriging method incorporating multiscale measurements in geochemical survey. *Journal of Geochemical Exploration*. 101: 147-154.

[68]. Daya, A.A. (2015). Application of median indicator kriging in the analysis of an iron mineralization. *Arabian Journal of Geosciences*. 8: 367-377.

[69]. Viswanathan, R., Jagan, J., Samui, P. and Porchelvan, P. (2015). Spatial Variability of Rock Depth Using Simple Kriging, Ordinary Kriging, RVM and MPMR. *Geotechnical and Geological Engineering*. 33: 69-78.

[70]. Vann, J. and Guibal, D. (1998). Beyond Ordinary Kriging—An overview of non-linear estimation,

Proceedings of a one day symposium: Beyond Ordinary Kriging.

[71]. Pokhrel, R.M., Kuwano, J. and Tachibana, S. (2013). A kriging method of interpolation used to map liquefaction potential over alluvial ground. *Engineering geology*. 152: 26-37.

[72]. Hu, H. and Shu, H. (2015). An improved coarse-grained parallel algorithm for computational acceleration of ordinary Kriging interpolation. *Computers & Geosciences*. 78: 44-52.

[73]. Cousineau, D. and Chartier, S. (2010). Outliers detection and treatment: a review. *International Journal of Psychological Research*. 3 (1): 58-67.

[74]. Costa, J.F. (2003). Reducing the impact of outliers in ore reserves estimation. *Mathematical geology*. 35: 323-345.

[75]. Schwertman, N.C., Owens, M.A. and Adnan, R. (2004). A simple more general boxplot method for identifying outliers. *Computational statistics & data analysis*. 47: 165-174.

[76]. Daya, A.A. and Bejari, H. (2015). A comparative study between simple kriging and ordinary kriging for estimating and modeling the Cu concentration in Chehlkureh deposit, SE Iran. *Arabian Journal of Geosciences*. 8: 6003-6020.

[77]. Carranza, E.J.M. (2011). Analysis and mapping of geochemical anomalies using logratio-transformed stream sediment data with censored values. *Journal of Geochemical Exploration*. 110: 167-185.

## کاربرد مدل‌سازی فرکتال برای تعیین زون‌های دگرسانی و واحدهای سنگ‌شناسی در نهشته پورفیری مس - طلا مسجد داغی، شمال غرب ایران

هانیه نیکوگفتار صفا و اردشیر هزارخانی\*

دانشکده مهندسی معدن و متالورژی، دانشگاه صنعتی امیرکبیر، ایران

ارسال ۲۰۱۸/۵/۱۱، پذیرش ۲۰۱۸/۷/۲۹

\* نویسنده مسئول مکاتبات: ardehez@aut.ac.ir

### چکیده:

در این پژوهش، مدل‌سازی کمی برای تعیین زون‌های دگرسانی و واحدهای سنگ‌شناسی در زون هیپوژن نهشته پورفیری مس - طلا مسجد داغی (شمال غرب ایران) بر اساس داده‌های مغزه حفاری ارائه شده است. هدف اصلی این پژوهش به کار بردن کریجینگ معمولی و مدل فرکتال غلظت - حجم بر اساس عیارهای مس به منظور جداسازی زون‌های دگرسانی و واحدهای سنگ‌شناسی مختلف است. در ابتدا، آنیزوتروپی بررسی و بر اساس محاسبه نیم- واریوگرام‌های تجربی عیارهای مس مدل شد و سپس جهات اصلی واریوگرافی شناسایی و ارزیابی شد. سپس، مدل بلوکی عیار مس با استفاده از کریجینگ تولید شد و تخمین به دست آمده از کریجینگ در مدل غلظت - حجم به کار برده شد. نمودار لگاریتم - لگاریتم غلظت - حجم مبتنی بر روش تخمین زون‌های دگرسانی و واحدهای سنگ‌شناسی مختلفی را از طریق مقادیر آستانه نشان داد. مقایسه و تفسیر زون‌های دگرسانی و واحدهای سنگ‌شناسی بر اساس مدل‌سازی فرکتال غلظت - حجم نشان داد که روش قابل قبول است و قادر به شناسایی درست زون‌های دگرسانی و واحدهای سنگ‌شناسی است. با توجه به همبستگی به دست آمده از ماتریس لگاریتم  $\log \text{ratio}$  (استفاده شده برای مقایسه مدل زمین‌شناسی با نتایج مدل فرکتال غلظت - مساحت)، مشاهده شد که مقادیر مس کمتر از ۰/۴ درصد به دست آمده از روش کریجینگ معمولی و کسل‌های همپوشانی با زون دگرسانی فیلپیک با صحت کلی ۰/۷۳۷ دارند. همبستگی فضایی بین زون دگرسانی پتاسیک به دست آمده از مدل‌سازی زمین‌شناسی سه بعدی و زون‌های غلظت بالا در مدل فرکتال غلظت - حجم مبتنی بر کریجینگ معمولی نشان داد که زون دگرسانی پتاسیک مطابق با مقادیر مس بالاتر از ۰/۴ درصد با صحت کلی ۰/۷۹۱ است. همچنین با استفاده از این روش، نتایج ارزشمندی برای واحدهای سنگی به دست آمد.

**کلمات کلیدی:** دگرسانی، کریجینگ معمولی، کریجینگ ساده، غلظت - حجم، نهشته مس مسجد داغی.